ChemistrySelect

Research Article
doi.org/10.1002/slct.202202069

Chemistry Europe
European Chemical Societies Publishing

www.chemistryselect.org

Medicinal Chemistry & Drug Discovery

# *In-silico* Computational Investigations of AntiViral Lignan Derivatives as Potent Inhibitors of SARS CoV-2

Dipen K. Sureja,*[a] Ashish P. Shah,[b] Normi D. Gajjar,[a] Shwetaba B. Jadeja,[a] Kunjan B. Bodiwala,[a] and Tejas M. Dhameliya*[a]

Due to alarming outbreak of pandemic COVID-19 in recent times, there is a strong need to discover and identify new antiviral agents acting against SARS CoV-2. Among natural products, lignan derivatives have been found effective against several viral strains including SARS CoV-2. Total of twenty-seven reported antiviral lignan derivatives of plant origin have been selected for computational studies to identify the potent inhibitors of SARS CoV-2. Molecular docking study has been carried out in order to predict and describe molecular interaction between active site of enzyme and lignan derivatives. Out of identified hits, clemastatin B and *erythro*-strebluslignanol G demonstrated stronger binding and high affinity with all selected proteins. Molecular dynamics simulation studies of clemastin B and savinin against promising targets of SARS CoV-2 have revealed their inhibitory potential against SARS CoV-2. In fine, *in-silico* computational studies have provided initial breakthrough in design and discovery of potential SARS CoV-2 inhibitors.

## Introduction

According to the World Health Organization (WHO), a pneumonia-like illness of unknown cause was detected in Wuhan city of China dated December 31, 2019. Later on, it was found to be caused by a new coronavirus which was identified as 2019 novel coronavirus (2019-nCoV), then renamed as severe acute respiratory syndrome coronavirus 2 (SARS CoV-2), and the disease was then named coronavirus disease 2019 (COVID-19). The WHO has declared this outbreak as a public health emergency of international concern and subsequently pandemic on January 30, and March 11, 2020, respectively.[1] According to WHO, there have been an estimated 543,352,927 cases and 6,331,059 deaths due to COVID-19 till June 29, 2022.[2] COVID-19 has led the world into a new era of recession by locking down the people in their homes through strict quarantines/isolations. The panic of COVID-19 has been more aggravated, wherein no therapeutic panacea for COVID-19 affected patients has been identified.[3–5]

Although no specific drugs have been approved by the United States Food and Drug Administration (USFDA) to treat COVID-19, several approaches have been proposed, such as lopinavir/ritonavir (400/100 mg, orally, twice a day), chloroquine (500 mg, orally, twice a day), and hydroxychloroquine (loading dose-400 mg, orally, twice a day followed by a maintenance dose of 200 mg, orally, twice a day). However, hydroxychloroquine and chloroquine show serious side effects like nausea, vomiting, diarrhea, and highly cardiotoxic effects like arrhythmia, hypokalemia, hypotension, etc.[6] As of April 21, 2020, more than 500 clinical trials have been registered worldwide in response to the COVID-19 emergency.[7] These clinical trials include efficacy evaluation of various drugs like favipiravir, a combination of hydroxychloroquine and azithromycin, remdesivir, IL-6 inhibitors (tocilizumab and sarilumab), etc. against SARS CoV-2 infection. However, to date, no new drug has been discovered and developed to treat COVID-19 disease as well the vaccines discovered against COVID-19[8] have not been found to offer life-long immunization.

The process of traditional drug discovery (also known as phenotypic) is highly laborious, risky, expensive, and time-consuming. Numerous strategies like computational chemistry, high throughput screening, fragment approaches, and -omics methodologies like functional and structural genomics, proteomics, metabolomics, etc.[7–10] can be utilized to accelerate the drug discovery process. Drug repositioning, repurposing, or reprofiling has been considered one of the best approaches to speed up the drug discovery process by identifying a novel therapeutic use of drugs previously approved by USFDA.[9] In the quick search of these agents, virtual screening of compounds has been identified as the most important and innovative approach.[10,11]

Several natural products have been reported as the therapeutic agents in treatment and management of SARS CoV-2.[12] Among these, lignan and its derivatives are of utmost importance due to their presence in highly diversified plant species. Lignans, secondary metabolites of plants, contain a basic scaffold of two or more phenylpropanoid units. Among the lignan derivatives, anti-neoplastic podophyllotoxin, and its

[a] *Dr. D. K. Sureja, N. D. Gajjar, S. B. Jadeja, Dr. K. B. Bodiwala, Dr. T. M. Dhameliya*
Department of Pharmaceutical Chemistry and Quality Assurance,
L. M. College of Pharmacy, Navrangpura,
Ahmedabad-380009, Gujarat, India
E-mail: dipensureja@gmail.com
tmdhameliya@gmail.com

[b] *Dr. A. P. Shah*
Department of Pharmacy, Sumandeep Vidyapeeth,
Vadodara-391760, Gujarat, India

Supporting information for this article is available on the WWW under https://doi.org/10.1002/slct.202202069

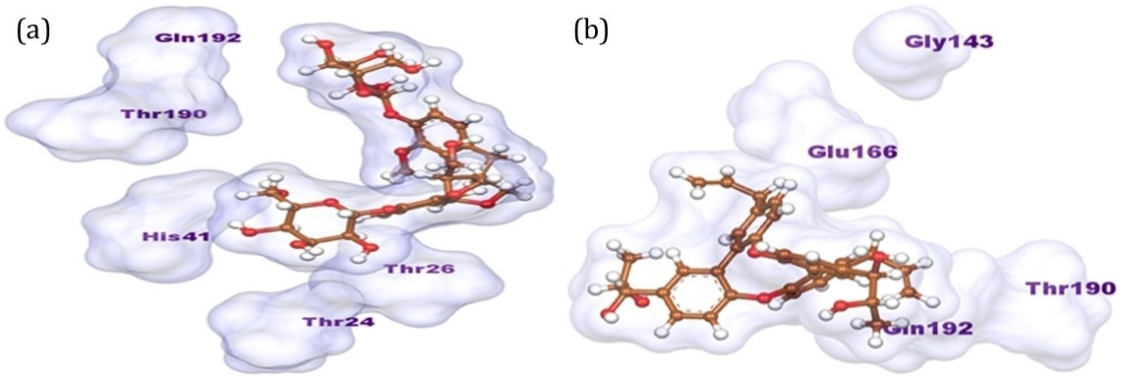


**Figure 1.** The 3D interactions of amino acid residues of main protease (PDB ID: 6M2N) with clemastatin B (**a**) and *erythro*-streblusligna nol G (**b**).

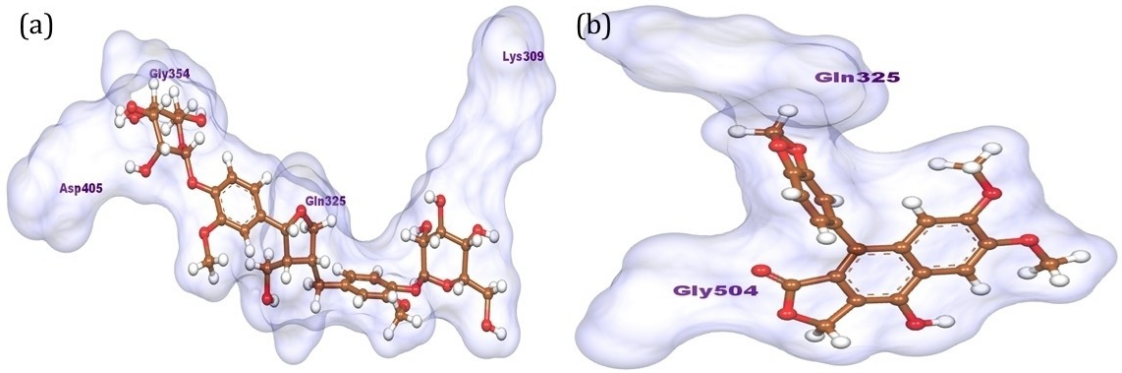


**Figure 2.** The 3D interactions of amino acid residues of spike glycoprotein with ACE-2 (PDB ID: 6LZG) with clemastatin B (**a**) and diphyllin (**b**).

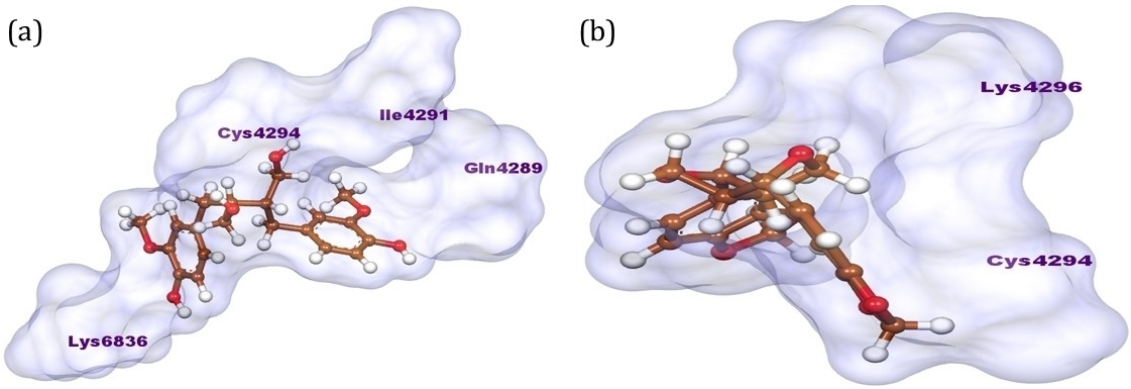


**Figure 3.** The 3D interactions of amino acid residues of non-structural proteins (PDB ID: 6W4H) with secoisolariciresinol (**a**) and sesamin (**b**).

synthetic derivatives, teniposide, and etoposide, have drawn significant attention in medicinal chemistry.[13] Further lignans have been identified as essential pharmacophoric features for diverse pharmacological activities such as anti-SARS-CoV,[14] antioxidant,[15] anti-inflammatory,[16] antimalarial,[17] and anticancer.[18] Lignans have also been found as the key scaffolds for antiviral activities among the diversely substituted natural products.[19,20]

In the absence of a specific SARS CoV-2 inhibitor, it is an urgent need of an hour to identify the repurposed drug for the treatment of COVID-19 during these extremely alarming situations. Keeping this in mind and continuing our research endeavour in search of newer SARS CoV-2 inhibitors,[21–23] we studied the potential of lignan derivatives as SARS CoV-2 inhibitors through *in-silico* based virtual screening, molecular dynamics (MD) simulations and druggability analysis.

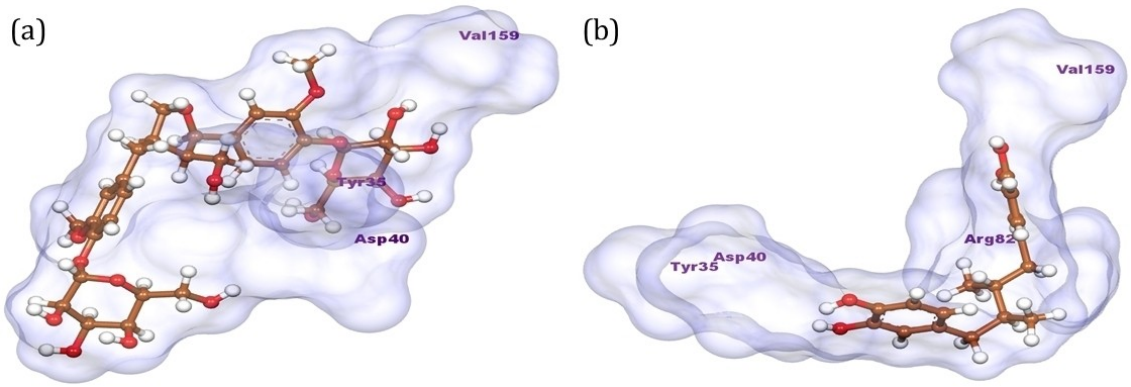


**Figure 4.** The 3D interactions of amino acid residues of papain-like protease (PDB ID: 6WRH) with clemastatin B **(a)** and nordihydroguaiaretic acid **(b)**.

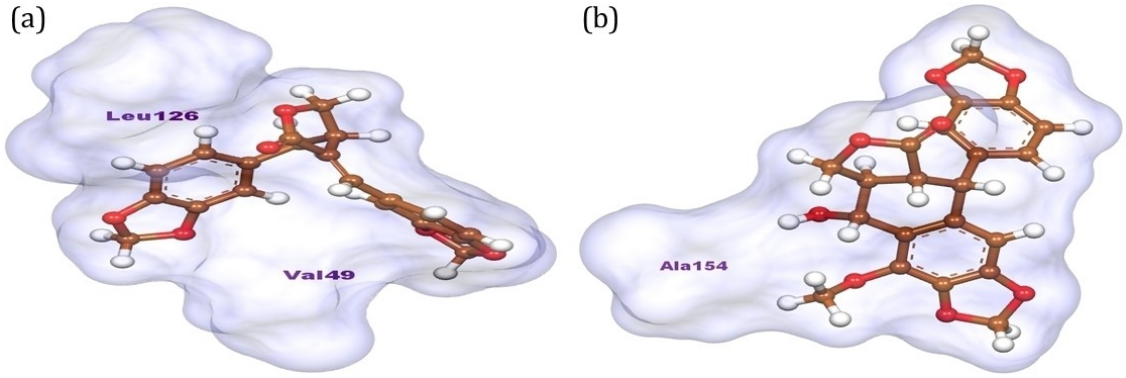


**Figure 5.** The 3D interactions of amino acid residues of papain-like protease (PDB ID: 6W6Y) with savinin (**a**) and cleistantoxin (**b**).

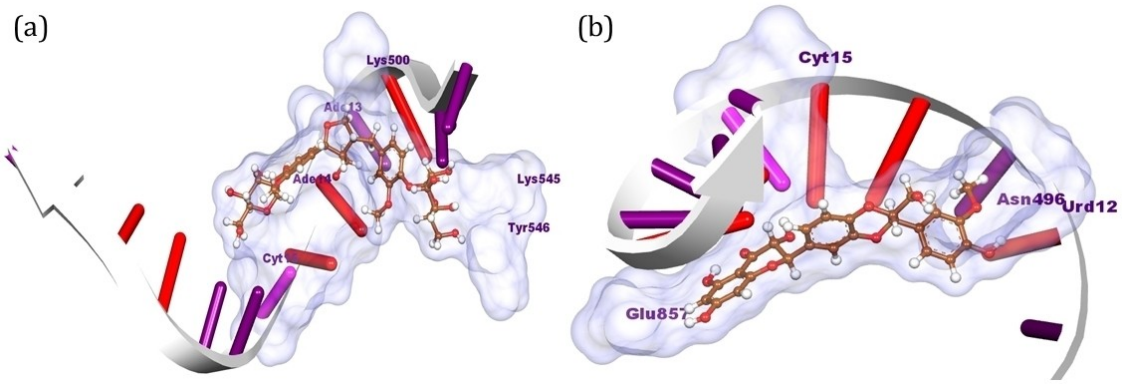


**Figure 6.** The 3D interactions of amino acid residues of RdRp (PDB ID: 7BV2) with clemastatin B (**a**) and silymarin (**b**).

## Results and Discussion

### Protein Structures and Ligands Selection

Following the literature search,[24] various enzymes like main protease/chymotrypsin-like protease (Mpro/3CLpro), papain-like protease (PLpro), surface spike glycoprotein with ACE-2 (S), RNA-dependent RNA polymerase (RdRp), and non-structural protein 16 (2′-O-methyltransferase, Nsp10/16) as targets for docking of lignan derivatives against SARS CoV-2 have been identified. In search of potent antiviral agents exhibiting multiple modes of action against different targets, virtual screening was performed using previously reported twenty-seven lignans (Table 1) as natural products against the selected enzymes (PDBs: 6M2N, 6W6Y, 6WRH, 6LZG, 7BV2, and 6W4H).

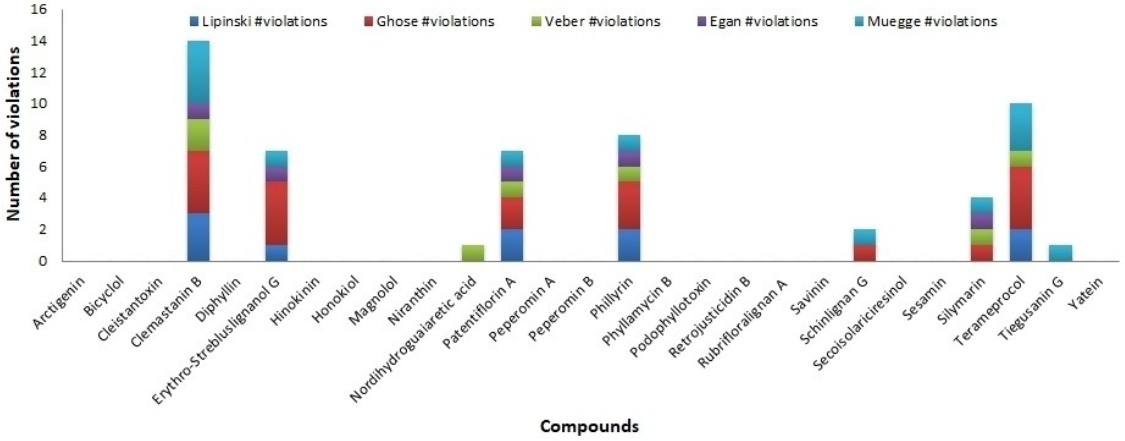


**Figure 7.** Result of the selected lignan derivatives against different violations for the rules of druggability and drug-likeness.

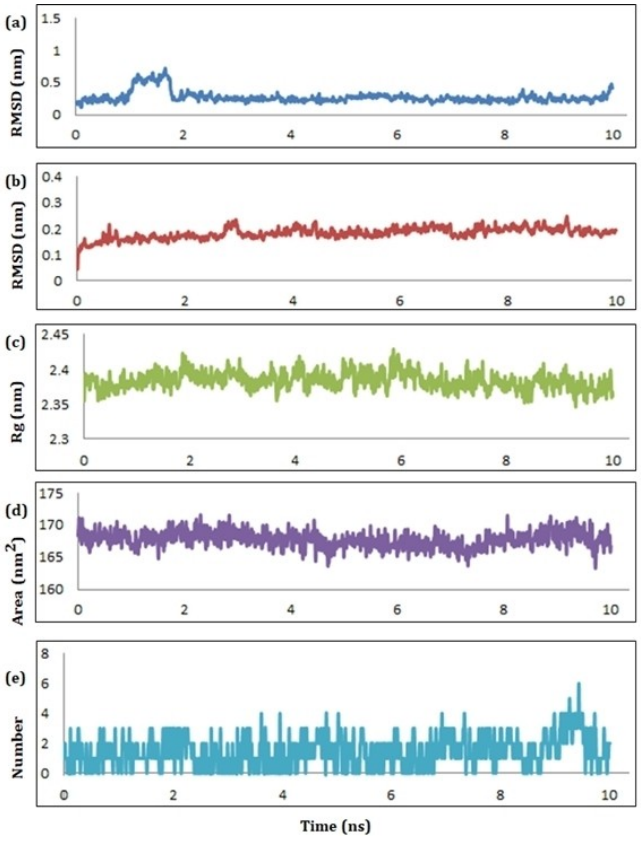


**Figure 8.** The schematic plots of RMSD–L (a), RMSD–P (b), RoG (c), SASA (d), and HB (e) for the complex of PLpro with clemastanin B.

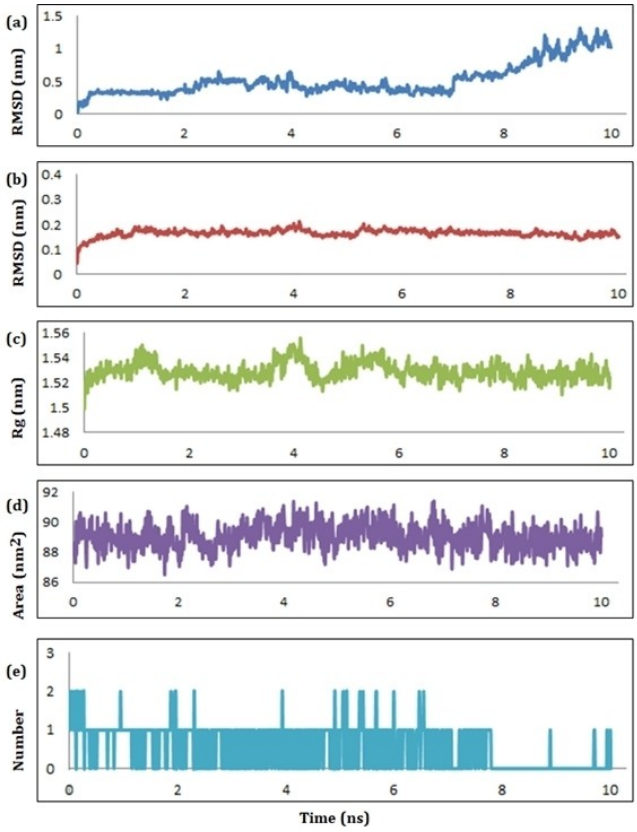


**Figure 9.** The schematic plots of RMSD–L (a), RMSD–P (b), RoG (c), SASA (d), and HB (e) for the complex of PLpro with savinin.

## Molecular Docking Studies

Molecular docking has been a type of structure-based drug design (SBDD) technique used to identify molecular interactions between the lowest energy conformations of molecules and amino acids of the selected protein. Maestro interface (Schrödinger Suite, LLC, NY) and Biovia Discovery studio were used to visualize and analyze the molecular interactions of docked ligands with proteins. A docking score was used to assess the binding affinity of the ligands with the receptor. Docking scores of the lignan derivatives and drugs like arbidol, lopinavir, and remdesivir with the selected PDBs have been described in Table 2. As per the obtained results in the molecular docking study, clemastanin B has got the highest docking score against four proteins (6M2N, 6LZG, 6WRH and

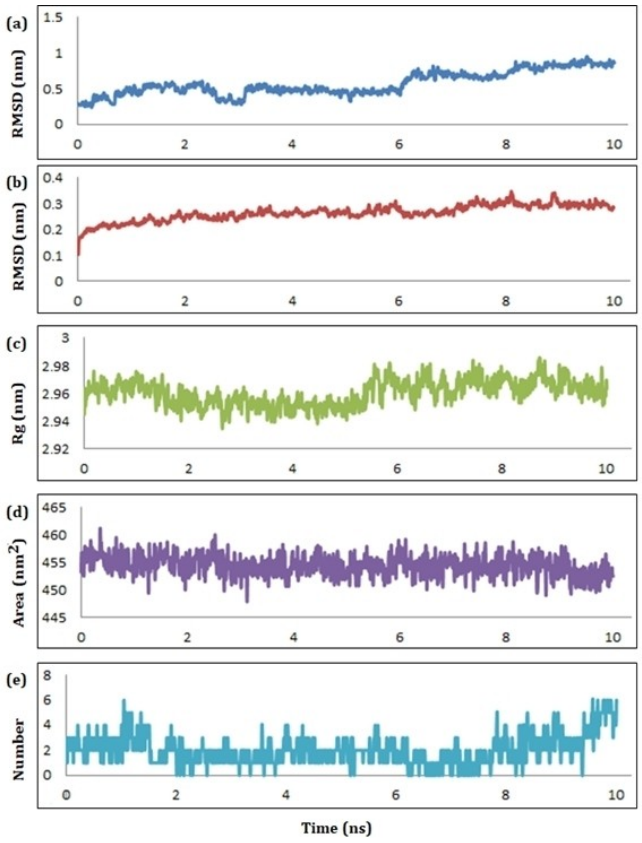


**Figure 10.** The schematic plots of RMSD–L (a), RMSD–P (b), RoG (c), SASA (d), and HB (e) for the complex of RdRp with clemastanin B.

7BV2) out of selected six proteins. These results show that Clemastanin B have the potential to inhibit multiple targets of the virus. Apart from this, cleistantoxin, diphyllin, silymarin, *erythro*-strebluslignanol G, hinokinin, arctigenin, peperomin A, and savinin also have the satisfactory docking score against the various targets.

Next, we studied the binding mode of the most potent compounds against the selected target and studied their interactions. The 3D poses generated using Biovia Discovery Studio[54] have been presented in the respective figures. Clemastanin B and *erythro*-strebluslignanol G have been identified as the hit molecules with the docking score of −8.19 and −7.50, respectively, against the SARS CoV-2 main protease (PDB ID: 6M2N). Due to multiple hydroxyl groups in the structure, clemastanin B forms hydrogen bonds (HB) with the amino acids Thr24, Thr26, His41, Thr190, and Gln192 (Figure 1a). Similarly, hydroxy groups of *erythro*-strebluslignanol G form HB with the amino acid residues Gly143, Glu166, Thr190, and Gln192 (Figure 1b).

Clemastanin B and diphyllin were found to inhibit the native spike protein with ACE-2 (PDB ID: 6LZG) with the docking score −6.17 and −5.82, respectively. Both lignans were found with superior docking scores than that of remdesivir (−5.41) and a comparable docking score to lopinavir (−6.56). The key residues such as Lys309, Gln325, and Gly354 from chain A and Asp405 from chain B were found to interact with the hydroxyl groups of the clemastanin B (Figure 2a). Whereas Gln325 residue from chain A forms HB with the ethereal oxygen and Gly504 residue from chain B forms HB with the ketones of diphyllin (Figure 2b).

Secoisolariciresinol and sesamin, with the respective docking scores of −5.44 and −5.34 against the non-structural proteins (nsp10 and nsp16) of the SARS CoV-2, found superior to remdesivir (docking score of −5.11) and highly significant than lopinavir (docking score of −3.69). Lys6836 residue of chain A and Gln4289, Ile4291, and Cys4294 residues of chain B were found to form HB with hydroxyl groups of the ligand secoisolariciresinol (Figure 3a). Ethereal oxygen of sesamin interacted through HB interactions with Cys4294 and Lys4296 residues of the chain B against the Nsp 10/16 (Figure 3b).

Clemastanin B and nordihydroguaiaretic acid were found to inhibit the papain-like protease enzyme (PDB ID: 6WRH) of the SARS CoV-2 with docking scores of −6.28 and −5.80, respectively. Their higher docking scores were quite good than remdesivir (−5.36) and comparable to lopinavir (−6.62). The hydroxy groups of the clemastanin B interacted by forming the HB with residues Tyr35, Asp40, and Val159 (Figure 4a). Total four hydroxy groups present in the nordihydroguaiaretic acid formed HB with Tyr35, Asp40, Arg82, and Val159 residues (Figure 4b).

Several heterocycles have been reported as anti-infectious agents against pathogemic microorganisms[55–59] with their greener synthesis.[60–63] Following this, heterocyclic ligands such as savinin and cleistantoxin showed the inhibition of papain-like protease (PDB ID: 6W6Y) with docking scores of −8.05 and −7.66, respectively, which are superior to the remdesivir (docking score of −7.37). In the savinin, ethereal oxygen formed HB with the amino acid Val49, and carbonyl oxygen formed HB with the residue Leu126 (Figure 5a). The hydroxyl group of cleistantoxin was found to form HB with the Ala154 amino acid (Figure 5b).

Clemastanin B with the docking score −6.89 inhibited the RNA replicase enzyme (PDB ID: 7BV2) more significantly than all the known inhibitors such as arbidol, lopinavir, and remdesivir. Nucleotides Ade13, Ade14, and Tyr546 (Chain A) formed HB with the hydroxy groups whereas, Cyt15 and Lys545 formed HB with ethereal oxygen. Along with this, Lys500 interacted with the π-cation interaction (Figure 6a). With the docking score of −4.93, hydroxy groups of the silymarin formed HB with the nucleotides (Urd12 and Cyt15) and amino acid residues of chain A (Asn496 and Glu857, Figure 6b). We did not observe a common interaction between the co-crystallized ligand, remdesivir and our identified hits including clemastatin B and silymarin in a common pocket occupied by them. However, clemastatin B has been found to interact with other nucleotide residues of the RdRp protein which can be attributed to its superior docking scores as compared to that of remdesivir.

## ADMET and Drug Likeliness Analysis

Next, we studied the Lipinski parameters for the selected hits to study their drug likeliness.[64] The physicochemical properties

**Table 1.** Antiviral lignan derivatives used for docking study in the present work.

| Compounds | IUPAC Name | Biological source (Family) | Active against[a] | Ref. |
|---|---|---|---|---|
| Arctigenin | (3*R*,4*R*)-4-(3,4-dimethoxybenzyl)-3-(4-hydroxy-3-methoxybenzyl)dihydrofuran-2(3*H*)-one | *Arctium lappa* (Compositae) | IAV<br>HIV-1 | [25] |
| Bicyclol (Synthetic analogue of Schizandrin C) | methyl 5′-(hydroxymethyl)-7,7′-dimethoxy-[4,4′-bibenzo[*d*][1,3]dioxole]-5-carboxylate | *Fructus Schisandrae* (Magnoliaceae) | ZIKV<br>HBV<br>HCV | [26] |
| Cleistantoxin | (5*R*,5a*R*,8a*R*,9*R*)-9-(1,3-benzodioxol-5-yl)-5-hydroxy-4-methoxy-5a,6,8a,9-tetrahydro-5*H*-[2]benzofuro[6,5-*f*][1,3]benzodioxol-8-one | *Cleistanthus indochinensis* (Euphorbiaceae) | Virus | [27] |
| Clemastanin B | 2-(hydroxymethyl)-6-(4-(3-(hydroxymethyl)-4-(3-methoxy-4-((3,4,5-trihydroxy-6-(hydroxymethyl)tetrahydro-2*H*-pyran-2-yl)oxy)benzyl)tetrahydrofuran-2-yl)-2-methoxyphenoxy)tetrahydro-2*H*-pyran-3,4,5-triol | *Isatis indigotica* (Cruciferae) | IAV | [28] |
| Diphyllin | 9-(benzo[*d*][1,3]dioxol-5-yl)-4-hydroxy-6,7-dimethoxynaphtho[2,3-*c*]furan-1(3H)-one | *Haplophyllum telephioides* (Rutaceae) | ZIKV<br>IAV | [29,30] |
| *Erythro*-Strebluslignanol G | 1,1′-(6,15-diallyltetrabenzo[*b*,*d*,*g*,*i*][1,6]dioxecine-3,12-diyl)bis(propane-1,2-diol) | *Streblus asper* (Moraceae) | HBV | [31] |
| Hinokinin | (3*R*,4*R*)-3,4-bis(1,3-benzodioxol-5-ylmethyl)oxolan-2-one | *Chamecyparis obtusa* (Cupressaceae) | SARS-CoV<br>HBV<br>HIV | [14,32,33] |
| Honokiol | 3′,5-diallyl-[1,1′-biphenyl]-2,4′-diol | *Magnolia officinalis* (Magnoliaceae) | SARS-CoV | [14] |
| Magnolol | 5,5′-diallyl-[1,1′-biphenyl]-2,2′-diol | *Magnolia officinalis* (Magnoliaceae) | SARS-CoV | [14] |
| Niranthin | 6-(3-(3,4-dimethoxybenzyl)-4-methoxy-2-(methoxymethyl)butyl)-4-methoxybenzo[*d*][1,3]dioxole | *Phyllanthus niruri* (Euphorbiaceae) | HBV | [32,34] |
| Nordihydroguaiaretic acid | 4,4′-(2,3-dimethylbutane-1,4-diyl)bis(benzene-1,2-diol) | *Larrea tridentate* (Zygophyllaceae) | DENV<br>HCV<br>WNV/ZIKV | [35–37] |
| Patentiflorin A | 9-(1,3-benzodioxol-5-yl)-6,7-dimethoxy-4-[(2*S*,3*R*,4*S*,5*S*,6*R*)-3,4,5-trihydroxy-6-methyloxan-2-yl]oxy-3*H*-benzo[*f*][2]benzofuran-1-one | *Justicia gendarussa* (Acanthaceae) | ZIKV<br>HIV-1 | [29,38] |
| Peperomin A | 4-(bis(7-methoxybenzo[*d*][1,3]dioxol-5-yl)methyl)-3-methyldihydrofuran-2(3*H*)-one | *Peperomia pellucida* (Piperaceae) | HIV-1 | [39] |
| Peperomin B | 4-((7-methoxybenzo[*d*][1,3]dioxol-5-yl)(3,4,5-trimethoxyphenyl)methyl)-3-methyldihydrofuran-2(3*H*)-one | *Peperomia pellucida* (Piperaceae) | HIV-1 | [39] |
| Phillyrin | 4-((1*S*,3a*R*,4*R*,6a*R*)-4-(3,4-dimethoxyphenyl)tetrahydro-1*H*,3*H*-furo[3,4-*c*]furan-1-yl)-2-methoxyphenol | *Fructus forsythiae* (Oleaceae) | IAV | [40] |
| Phyllamycin B | 1-(1,3-benzodioxol-5-yl)-6,7-dimethoxy-3-(methoxymethyl)naphthalene-2-carbaldehyde | *Phyllanthus myrtifolius* (Phyllanthaceae) | HIV-1 | [41] |
| Podophyllotoxin | (5*R*,5a*R*,8a*R*,9*R*)-9-hydroxy-5-(3,4,5-trimethoxyphenyl)-5,8,8a,9-tetrahydrofuro[3′,4′:6,7]naphtho[2,3-*d*][1,3]dioxol-6(5a*H*)-one | *Podophyllum peltatum* (Berberidaceae) | HSV<br>IAV<br>HIV | [42] |
| Retrojusticidin B | 4-(1,3-benzodioxol-5-yl)-6,7-dimethoxy-3*H*-benzo[*f*][2]benzofuran-1-one | *Phyllanthus myrtifolius* (Phyllanthaceae) | HIV-1 | [41] |
| Rubrifloralignan A | (9*R*,10*S*)-4,5,14,15-tetramethoxy-9,10-dimethyltricyclo[10.4.0.02,7]hexadeca-1(16),2,4,6,12,14-hexaene-3,16-diol | *Schisandra rubriflora* (Schisandraceae) | HIV-1 | [43] |
| Savinin | (*R*,*E*)-4-(benzo[*d*][1,3]dioxol-5-ylmethyl)-3-(benzo[*d*][1,3]dioxol-5-ylmethylene)dihydrofuran-2(3*H*)-one | *Chamaecyparis obtuse* (Cupressaceae) | SARS-CoV | [14] |
| Schinlignan G | (7*R*)-2,3,10,11,12-pentamethoxy-6,7-dimethyl-5,6,7,8-tetrahydrodibenzo[*a*,*c*][8]annulen-1-yl methacrylate | *Schisandra chinensis* (Schisandraceae) | HBV | [44] |
| Secoisolariciresinol | (2*R*,3*R*)-2,3-bis(4-hydroxy-3-methoxybenzyl)butane-1,4-diol | *Justicia procumbens* (Acanthaceae) | HIV-1 | [45] |
| Sesamin | (1*S*,3a*R*,4*S*,6a*R*)-1,4-bis(benzo[*d*][1,3]dioxol-5-yl)tetrahydro-1*H*,3*H*-furo[3,4-*c*]furan | *Sesamum indicum* (Pedaliaceae) | H1 N1 | [46] |
| Silymarin | (2*R*,3*R*)-3,5,7-trihydroxy-2-[(2*R*,3*R*)-3-(4-hydroxy-3-methoxyphenyl)-2-(hydroxymethyl)-2,3-dihydro-1,4-benzodioxin-6-yl]-2,3-dihydrochromen-4-one | *Silybum marianum* (Compositae) | HCV<br>IAV | [47,48] |
| Terameprocol | 4,4′-(2,3-dimethylbutane-1,4-diyl)bis(1,2-dimethoxybenzene) | *Larrea tridentate* (Zygophyllaceae) | WNV/ZIKV<br>Poxvirus HSV<br>HIV<br>HPV | [37,49–51] |
| Tiegusanin G | [(8*S*,9*S*,10*S*,11*R*)-9-hydroxy-3,4,5,19-tetramethoxy-9,10-dimethyl-11-[(*E*)-3-phenylprop-2-enoyl]oxy-15,17-dioxatetracyclo[10.7.0.02,7.014,18]nonadeca-1(19),2,4,6,12,14(18)-hexaen-8-yl] (*Z*)-2-methylbut-2-enoate | *Schisandra propinqua* (Schisandraceae) | HIV-1 | [52] |
| Yatein | (3*R*,4*R*)-4-(benzo[*d*][1,3]dioxol-5-ylmethyl)-3-(3,4,5-trimethoxybenzyl)dihydrofuran-2(3*H*)-one | *Chamaecyparis obtuse* (Cupressaceae) | HSV-1 | [53] |

[a] DENV-Dengue Virus; H1N1-Influenza A virus subtype H1N1; HBV-Hepatitis B Virus; HCV-Hepatitis C Virus, HIV-Human Immunodeficiency Virus, HIV-1-Human Immunodeficiency Virus-1; HPV-Human Papilloma Virus; HSV-Herpes Simplex Virus; HSV-1-Herpes Simplex Virus-1; IAV-Influenza A Virus; SARS-CoV-Severe Acute Respiratory Syndrome-related Corona Virus; WNV-West Nile Virus; ZIKV-Zika Virus.

like logP (−5 to 5), molecular weight (less than 500 Dalton), H-bond donors (less than 10), and H-bond acceptors (less than 5) of the drug molecules have close resemblance with the oral bioavailability of a drug.[64] The polar surface area (7–200 Å$^2$)

**Table 2.** Docking score of lignan derivatives with different PDBs.

| Compound | Mpro (6M2N) | Spike glycoprotein (6LZG) | Nsp 10/16 (6W4H) | PLpro (6WRH) | PLpro (6W6Y) | RdRp (7BV2) |
|---|---|---|---|---|---|---|
| Arctigenin | −6.00 | −3.63 | −4.63 | **−5.35** | **−7.12** | −3.62 |
| Bicyclol | −6.16 | −4.52 | −4.15 | −4.21 | −6.10 | −3.11 |
| Cleistantoxin | −5.60 | −4.42 | −2.90 | −3.76 | **−7.66** | −2.95 |
| Clemastanin B | **−8.19** | **−6.17** | – | **−6.28** | −5.90 | **−6.89** |
| Diphyllin | −6.59 | **−5.82** | −4.23 | −3.25 | −6.68 | −3.41 |
| *Erythro*-Streblusliganol G | **−7.50** | **−5.53** | **−5.30** | −4.71 | −6.63 | **−4.71** |
| Hinokinin | **−7.29** | **−4.95** | **−4.85** | −5.10 | −6.91 | −2.84 |
| Honokiol | −6.31 | −4.30 | −3.83 | – | – | −3.64 |
| Magnolol | −5.14 | −4.29 | −3.51 | −3.99 | −5.15 | **−4.55** |
| Niranthin | −6.86 | −4.14 | −4.35 | −5.09 | −6.41 | −2.97 |
| Nordihydroguaiaretic acid | −6.74 | −4.18 | −4.14 | **−5.80** | **−7.36** | −4.21 |
| Patentiflorin A | **−7.37** | −4.20 | – | −3.94 | −5.72 | −3.73 |
| Peperomin A | – | −3.99 | **−5.00** | **−5.35** | **−7.55** | −3.27 |
| Peperomin B | −6.54 | −4.05 | −4.78 | **−5.78** | −5.94 | −3.60 |
| Phillyrin | −5.94 | −3.84 | – | −4.56 | −4.45 | −3.64 |
| Phyllamycin B | −6.72 | **−5.11** | – | −4.35 | −6.19 | −3.56 |
| Podophyllotoxin | −5.90 | −4.20 | −2.77 | −4.33 | −5.20 | −3.32 |
| Retrojusticidin B | −6.25 | −4.51 | −4.22 | −5.04 | −6.18 | −3.11 |
| Rubrifloralignan A | −5.47 | −3.22 | −3.52 | −4.38 | −4.92 | −2.85 |
| Savinin | **−7.36** | −4.74 | **−4.89** | −4.97 | **−8.05** | −3.80 |
| Schinlignan G | −5.34 | −3.63 | −3.41 | −2.70 | −5.91 | −3.62 |
| Secoisolariciresinol | −5.36 | −3.33 | **−5.44** | −4.26 | **−7.54** | −3.50 |
| Sesamin | −6.86 | −4.69 | **−5.34** | −5.22 | −5.79 | −3.16 |
| Silymarin | −6.75 | −3.62 | −4.18 | −5.31 | −5.90 | **−4.93** |
| Terameprocol | −6.57 | −4.36 | −4.12 | −5.15 | −6.50 | −3.11 |
| Tiegusanin G | −0.1 | −0.76 | −0.82 | −3.76 | −3.67 | −3.21 |
| Yatein | −6.24 | −4.58 | −3.24 | −5.04 | −7.04 | −4.10 |
| Arbidol | −5.99 | −3.34 | −3.30 | −3.28 | −3.91 | −2.72 |
| Lopinavir | **−8.70** | **−6.56** | −3.69 | **−6.62** | −6.27 | **−5.51** |
| Remdesivir | **−8.65** | **−5.41** | **−5.11** | **−5.36** | **−7.37** | **−6.02** |

**Table 3.** Calculated physicochemical properties of lignan derivatives.

| Compound | MW[a] | QPlogPo/w[b] | HBA[c] | HBD[d] | RB[e] | PSA[f] | Lipinski violations |
|---|---|---|---|---|---|---|---|
| Arctigenin | 372.42 | 3.54 | 6 | 1 | 7 | 85.69 | 0 |
| Bicyclol | 390.35 | 2.25 | 9 | 1 | 6 | 107.69 | 0 |
| Cleistantoxin | 398.37 | 1.79 | 8 | 1 | 2 | 102.84 | 0 |
| Clemastanin B | 684.69 | −1.57 | 16 | 9 | 12 | 240.49 | 3 |
| Diphyllin | 380.35 | 2.58 | 7 | 1 | 3 | 95.13 | 0 |
| ***Erythro*-Streblusliganol G** | 564.68 | 5.86 | 6 | 4 | 8 | 95.50 | 2 |
| Hinokinin | 354.36 | 2.49 | 6 | 0 | 4 | 77.63 | 0 |
| Honokiol | 266.34 | 4.97 | 2 | 2 | 5 | 40.65 | 0 |
| Magnolol | 266.34 | 4.96 | 2 | 2 | 5 | 40.65 | 0 |
| Niranthin | 432.51 | 3.27 | 7 | 0 | 12 | 58.60 | 0 |
| Nordihydroguaiaretic acid | 302.37 | 2.61 | 4 | 4 | 5 | 88.43 | 0 |
| Patentiflorin A | 526.50 | 1.32 | 11 | 3 | 5 | 151.61 | 2 |
| Peperomin A | 414.41 | 2.62 | 8 | 0 | 5 | 94.11 | 0 |
| Peperomin B | 430.45 | 3.36 | 8 | 0 | 7 | 90.30 | 0 |
| Phillyrin | 534.56 | 1.46 | 11 | 4 | 8 | 140.92 | 2 |
| Phyllamycin B | 380.40 | 3.21 | 6 | 0 | 6 | 74.55 | 0 |
| Podophyllotoxin | 414.41 | 2.45 | 8 | 1 | 4 | 101.16 | 0 |
| Retrojusticidin B | 364.35 | 2.76 | 6 | 0 | 3 | 76.63 | 0 |
| Rubrifloralignan A | 388.46 | 4.35 | 6 | 2 | 4 | 68.97 | 0 |
| Savinin | 352.34 | 2.12 | 6 | 0 | 3 | 77.94 | 0 |
| Schinlignan G | 470.56 | 5.52 | 7 | 0 | 8 | 65.59 | 1 |
| Secoisolariciresinol | 362.42 | 2.35 | 6 | 4 | 9 | 102.03 | 0 |
| Sesamin | 354.36 | 1.65 | 6 | 0 | 2 | 54.96 | 0 |
| Silymarin | 482.44 | 1.82 | 10 | 4 | 4 | 167.20 | 0 |
| Terameprocol | 358.48 | 5.26 | 4 | 0 | 9 | 31.36 | 1 |
| Tiegusanin G | 660.72 | 7.37 | 11 | 1 | 11 | 122.69 | 3 |
| Yatein | 400.43 | 3.67 | 7 | 0 | 7 | 82.12 | 0 |

[a]MW: Molecular weight, [b]QPlogPo/w: Partition coefficient, [c]HBA: Hydrogen bond donors; [d]HBD: Hydrogen bond donors; [e]RB: Rotational bonds; [f]PSA: Polar surface area.

**Table 4.** Predicted absorption and distribution properties of selected lignans using pkCSM.[a]

| Compound | Ali log S[b,c] | MR[b,d] | CaCO-2 permeability[e] | Human intestinal absorption (% absorbed)[f] | $VD_{ss}$ (Human)[g] | Fraction unbound (Human)[h] | P-gp inhibition (yes/no)[i] |
|---|---|---|---|---|---|---|---|
| Arctigenin | −4.84 | 100.6 | 1.27 | 96.65 | −0.50 | 0 | Yes |
| Bicyclol | −3.85 | 94.4 | 1.518 | 100 | −0.38 | 0.09 | No |
| Cleistantoxin | −3.62 | 96.93 | 1.69 | 100 | −0.58 | 0.07 | No |
| Clemastanin B | −3.48 | 161.34 | −0.98 | 5.04 | −0.23 | 0.25 | No |
| Diphyllin | −5.06 | 99.78 | 1.17 | 96.50 | −0.90 | 0.10 | Yes |
| *Erythro*-Strebluslignanol G | −8.12 | 165.92 | 0.26 | 100 | −1.90 | 0.32 | Yes |
| Hinokinin | −4.67 | 91.23 | 1.00 | 98.59 | −0.34 | 0 | Yes |
| Honokiol | −5.57 | 84.14 | 1.73 | 91.94 | 0.50 | 0 | No |
| Magnolol | −5.57 | 84.14 | 1.62 | 92.67 | 0.36 | 0.03 | No |
| Niranthin | −5.72 | 88.02 | 0.95 | 88.44 | 0.25 | 0.23 | No |
| Nordihydroguaiaretic acid | −5.14 | 117.25 | 1.27 | 100 | −0.10 | 0 | Yes |
| Patentiflorin A | −4.95 | 130.74 | 0.53 | 89.02 | −1.42 | 0.08 | Yes |
| Peperomin A | −5.03 | 104.21 | 1.31 | 100 | −0.51 | 0.07 | No |
| Peperomin B | −5.17 | 111.13 | 1.35 | 100 | −0.42 | 0.04 | No |
| Phillyrin | −2.64 | 131.49 | 0.24 | 58.24 | −0.88 | 0.09 | No |
| Phyllamycin B | −4.69 | 104.68 | 1.08 | 100 | −0.27 | 0.15 | Yes |
| Podophyllotoxin | −3.58 | 103.85 | 0.08 | 100 | −0.42 | 0 | Yes |
| Retrojusticidin B | −5.01 | 97.76 | 1.11 | 99.93 | −0.28 | 0.16 | Yes |
| Rubrifloralignan A | −5.96 | 108.94 | 1.15 | 96.56 | 0.38 | 0.05 | Yes |
| Savinin | −4.64 | 91.54 | 1.09 | 98.79 | −0.17 | 0 | No |
| Schinlignan G | −7.3 | 132.02 | 1.33 | 100 | −0.04 | 0 | No |
| Secoisolariciresinol | −4.25 | 99.28 | 1.09 | 67.35 | −0.17 | 0.12 | Yes |
| Sesamin | −3.5 | 90 | 1.17 | 98.22 | −0.34 | 0.04 | No |
| Silymarin | −4.78 | 120.55 | 0.25 | 66.91 | −0.58 | 0 | Yes |
| Terameprocol | −8.58 | 177.51 | 1.04 | 100 | −0.95 | 0.08 | Yes |
| Tiegusanin G | −6.15 | 105.90 | 1.07 | 96.30 | 0.39 | 0 | Yes |
| Yatein | −4.96 | 104.64 | 1.22 | 98.83 | −0.53 | 0 | Yes |

[a] Parameters calculated using pkCSM[67,68], [b] AlilogS and MR were calculated using SwissADME[69], [c] Aqueous solubility descriptor ($\leq 0$), [d] molar refractivity ($\leq 155$), [e] Caco-2 cell permeability (log Papp in $10^{-6}$ cm/s $> 0.09$), [f] absorption (human, % $> 30$), [g] volume of distribution (human, log L/kg) (low if $< -0.15$ and high if $> 0.45$), [h] fraction unbound, and [i] ability to inhibit the P-glycoprotein.

and rotatable bonds (0-15) present in the molecule also plays a vital role in the oral bioavailability of the drug.[65] The essential parameters with their results obtained from Qikprop have been presented in Table 3. As per Lipinski's rule of five, a maximum of two violations is allowed for an orally active compound. Most of the identified hits successfully passed the Lipinski filters with the good oral bioavailability within the permissible limits except clemastanin B and tiegusanin G. However, about half of united states food and drug administration (USFDA) approved drugs do not comply with rule along with the marketed natural products and their semisynthetic derivatives.[66] Hence, the strict adherence to Lipinski's rule of five should not be a limiting factor for the search of potent SARS CoV-2 inhibitors.

Next, we have analyzed several ADMET (absorption, distribution, metabolism, excretion and toxicity) parameters such as water solubility (Ali log S), molar refractivity (MR), CaCO-2 cell permeability, intestinal absorption, volume of distribution ($V_d$), unbound fraction of drug and ability to inhibit the P-glycoprotein substrate for the identified hits (Table 4). Most of the molecules have qualified with all the required criteria. Sufficient human intestinal absorption indicated their better oral bioavailability along with desired values of $V_d$. Further, we analyzed the additional parameters to predict the metabolism, excretion and toxicity profile (Table 5). None of the ligands except niranthin and sisamin was not found to inhibit the CYP2D6 metabolic enzymes. However, some of the compounds were found to inhibit the metabolic enzyme, CYP3A4 and P-glycoprotein substrate, indicating the need of reduction in dosages of these agents. They have medium renal clearance along with no ability of inhibiting the substrates for renal uptake transporter in proximal convoluted tubule (OCT2). All the molecules were found nontoxic from there toxicity profile like cytotoxicity (hERG cell line) and dermal toxicity (skin sensitization) and also found safe in terms of oral rat acute ($LD_{50}$), and chronic (LOAEL) toxicity. Hence, these compounds might be good and successful drug candidates in the future. The analysis of AMES toxicity revealed their non-mutagenic nature except bicyclol, retrojusticidin B and sesamin.

Apart from Lipinski's rule of 5, additional rules for the drug-likeliness such as Ghose rule, Veber's rule, Egan's rule and Muegge's rule have been also studied and the results have been analyzed to ensure the drug-likeliness of selected lignan derivatives (Figure 7). As per the Veber's rule, compound should have the polar surface area less than 140 $Å^2$ to have the better oral bioavailability.[70] Seven compounds out of the twenty-seven have found violated Veber's rule indicating good oral bioavailability of others. All hits except six qualified the criteria provided by the Egan rule [tPSA (0–132 $Å^2$) and logP

**Table 5.** Metabolism, excretion and safety parameters of selected lignans.[a]

| Compound | CYP2D6 Inhibitor[b] | CYP3A4 inhibitor[c] | $CL_T$[d] | Renal OCT2 substrate[e] | AMES toxicity[f] | hERG I toxicity[g] | $LD_{50}$[h] | LOAEL[i] | Skin sensitization[j] |
|---|---|---|---|---|---|---|---|---|---|
| Arctigenin | No | Yes | 0.22 | No | No | No | 2.11 | 1.47 | No |
| Bicyclol | No | No | 0.57 | No | Yes | No | 3.02 | 1.10 | No |
| Cleistantoxin | No | No | −0.01 | No | No | No | 2.96 | 1.11 | No |
| Clemastanin B | No | No | 0.52 | No | No | No | 2.78 | 4.64 | No |
| Diphyllin | No | Yes | 0.31 | No | No | No | 2.52 | 0.65 | No |
| *Erythro*-Strebluslignanol G | No | No | 0.29 | No | No | No | 2.84 | 2.76 | No |
| Hinokinin | No | Yes | −0.07 | No | No | No | 2.72 | 1.44 | No |
| Honokiol | No | No | 0.32 | No | No | No | 1.89 | 1.76 | No |
| Magnolol | No | No | 0.37 | No | No | No | 2.00 | 1.99 | No |
| Niranthin | Yes | No | −0.04 | No | No | No | 2.45 | 1.33 | No |
| Nordihydroguaiaretic acid | No | Yes | 0.47 | No | No | No | 2.57 | 1.45 | No |
| Patentiflorin A | No | No | 0.01 | No | No | No | 2.96 | 3.35 | No |
| Peperomin A | No | Yes | 0.02 | No | No | No | 3.24 | 1.09 | No |
| Peperomin B | No | Yes | 0.20 | No | No | No | 3.01 | 1.10 | No |
| Phillyrin | No | No | 0.56 | No | No | No | 2.89 | 3.12 | No |
| Phyllamycin B | No | Yes | 0.24 | No | No | No | 2.85 | 0.78 | No |
| Podophyllotoxin | No | Yes | 0.21 | No | No | No | 2.51 | 1.04 | No |
| Retrojusticidin B | No | Yes | 0.29 | No | Yes | No | 2.88 | 0.44 | No |
| Rubrifloralignan A | No | Yes | 0.18 | No | No | No | 2.31 | 1.89 | No |
| Savinin | No | Yes | 0.19 | No | No | No | 2.59 | 1.54 | No |
| Schinlignan G | No | Yes | 0.62 | No | No | No | 2.97 | 1.38 | No |
| Secoisolariciresinol | No | Yes | 0.25 | No | No | No | 1.81 | 1.64 | No |
| Sesamin | Yes | Yes | −0.10 | No | Yes | No | 2.78 | 1.55 | No |
| Silymarin | No | Yes | −0.08 | No | No | No | 2.56 | 3.40 | No |
| Terameprocol | No | Yes | 0.07 | No | No | No | 2.88 | 1.04 | No |
| Tiegusanin G | No | Yes | 0.23 | No | No | No | 2.27 | 1.99 | No |
| Yatein | No | Yes | 0.11 | No | No | No | 2.51 | 1.51 | No |

[a] Parameters calculated using pkCSM[67], [b] ability to inhibit CYP2D6 enzyme, [c] ability to inhibit CYP3 A4 enzyme, [d] total renal clearance; high ($>1$ mL/min/kg), medium ($>0.1$ to $<1$ mL/min/kg) or low ($\leq 0.1$ mL/min/kg), [e] ability to inhibit renal OCT2 substrate; [f] AMES toxicity; [g] hERG I toxicity; [h] oral rat acute toxicity ($LD_{50}$); [i] oral rat chronic toxicity (LOAEL); [j] skin sensitisation.

(−1 to 6)].[71] Muegge's filter includes several parameters for confirming the dug likeliness such as MW (200–600), lipophilicity (XLOGP3, −2 to 5), tPSA ($\leq 150$), cyclic rings ($\leq 7$), carbon atoms ($>4$), heteroatoms ($>1$), RB ($\leq 15$), HBA ($\leq 10$), and HBD ($\leq 5$)[72] and nine compounds were found to violate it. Ghose rule specified the desired requirements of MW (160—480 Da), LogP (−0.4 to 5.6), MR (40-130) and atoms (20–70) to be the good drug candidate[73] and eight molecules were violated this rule. Being phytochemicals, most of the selected lignan derivatives have potential to become the good drug candidate requiring further modifications through pharmacokinetic analysis and or QSAR.

## MD Simulation

With a view of exploring the stability of ligand into the active site of protein through various statistical parameters, molecular dynamics (MD) simulations[74,75] were carried out for 10 ns.[76–81] The hit complexes obtained from docking analysis were incorporated for MD simulations at various time points up to 10 ns using GROMACS 2020.1.[82,83] MD simulation was performed for complexes of Mpro with clemastanin B, spike glycoprotein with clemastanin B, Nsp 10/16 with secoisolariciresinol, PLpro with clemastanin B/savinin, and RdRp with clemastanin B. The graphical representation of plots for the MD simulations of the complex of PLpro with clemastanin B have been presented in Figure 8. The complex of clemastanin B with PLpro was found with a root mean square deviation (RMSD) of an average of 0.273 nm (Figure 8a) for the ligand and 0.182 nm (Figure 8b) for the protein indicating the stability of the ligand without significant deviation in the binding site. The radius of gyration (RoG) ranging from 2.34 to 2.42 nm with an average of 2.383 nm (Figure 8c) showed the compactness of the present complex. The surface area accessed by the solvent molecules (SASA) was found within the acceptable range from 164–172 $nm^2$ with an average of 167.79 $nm^2$ (Figure 8d). Maximum six hydrogen bonds (HB) were observed between the ligand and receptor from the plot of the number of HB *vs.* time. (Figure 8e). The average short-range Coulombic interaction energy (Coul-SR) was $-78.69 \pm 10$ kJ $mol^{-1}$. The short-range Lennard-Jones energy (LJ-SR) was $-104.93 \pm 1.8$ kJ $mol^{-1}$ indicating the significant contribution from van der Waals/Hydrophobic interactions over for electrostatic interactions.

RMSD values with an average of 0.522 nm (ligand, Figure 9a) and 0.165 nm (protein, Figure 9b) have been observed for the complex of savinin with PLpro, indicating enough stability of the ligand. The RoG was found in the range of 1.5–1.55 nm with an average of 1.529 nm (Figure 9c) supported the

compactness of this complex. The SASA ranged from 86–91 $nm^2$ with an average of 89.061 $nm^2$ (Figure 9d), and the plot of numbers of HB *vs.* run times showed a maximum of two HBs were formed between the ligand and receptor within the simulation time of 10 ns (Figure 9e). The Coul-SR and LJ-SR were observed were $-37.41 \pm 7.6$ kJ $mol^{-1}$ and $-102.41 \pm 11$ kJ $mol^{-1}$, respectively, indicating the pivotal role of hydrophobic or van der Waals to stabilize the complex.

Further, clemastanin B also has satisfactory stability in the active site of the RdRp with the stable RMSD observed with an average of 0.571 nm and 0.264 nm for the ligand and protein, respectively (Figure 10a and Figure 10b). The compactness of the complex was claimed by the slightest fluctuation in the RoG plot ranging from 2.93–2.99 nm with an average value of 2.960 nm (Figure 10c). The SASA in the range of 449–462 $nm^2$ with an average of 454.449 $nm^2$ (Figure 10d) and a maximum of six HB(Figure 10e) were observed for the said complex during the MD run. The average short-range Coulombic interaction energy (Coul-SR) with $-79.68 \pm 20$ kJ $mol^{-1}$ and the short-range Lennard-Jones energy (LJ-SR) with $-74.20 \pm 3.2$ kJ $mol^{-1}$ confirmed the stabilization of the complexes driven by electrostatic forces over van der Waals/Hydrophobic interactions, respectively.

## Conclusions

The present *in-silico* computational studies have revealed the naturally occurring lignans and their derivatives having remarkable efficacy and potency against SARS CoV-2. Among these lignans, clemastatin B, cleistantoxin, diphyllin, silymarin, *erythro*-strebluslignanol G, hinokinin, arctigenin, peperomin A, and savinin have been identified with suitable binding affinity and potential to inhibit SARS CoV-2 having a scope of fewer side effects being phytochemical constituents. Clemastanin B and savinin have been found with good stability, satisfactory compactness and reliable uniqueness at the active site of the promising targets during their MD simulations, warranting their strong candidature for further study. In fine, these studies have revealed the phytochemical inhibitors of SARS CoV-2 with the potential of inhibiting the promising viral proteins to fight against the deadly disease COVID-19.

## Supporting Information Summary

Supporting information comprises of experimental procedures adopted for molecular docking, ADMET, MD simulations along with representative 2-dimensional poses of hits with their docked complexes.

## *Acknowledgements*

*The authors acknowledge Schrödinger Inc. for providing a fully functional evaluation version to carry out molecular docking studies.*

## *Conflict of Interest*

The authors declare no competing financial interest.

## Data Availability Statement

The data that support the findings of this study are available in the supplementary material of this article.

**Keywords:** COVID-19 · Docking · Lignan · SARS CoV-2 · MD simulations

[1] H. Harapan, N. Itoh, A. Yufika, W. Winardi, S. Keam, H. Te, D. Megawati, Z. Hayati, A. L. Wagner, M. Mudatsir, *J. Infect. Public Health* **2020**, *13*, 667–673.
[2] "WHO Coronavirus Disease (COVID-19) Dashboard," can be found under https://covid19.who.int/, (accessed on Jun 30, **2022**).
[3] J. S. Morse, T. Lalonde, S. Xu, W. R. Liu, *ChemBioChem* **2020**, *21*, 730–738.
[4] C. Liu, Q. Zhou, Y. Li, L. V. Garner, S. P. Watkins, L. J. Carter, J. Smoot, A. C. Gregg, A. D. Daniels, S. Jervey, D. Albaiu, *ACS Cent. Sci.* **2020**, *6*, 315–331.
[5] Shagufta, I. Ahmad, *Eur. J. Med. Chem.* **2021**, *213*, 113157.
[6] R. C. Becker, *J. Thromb. Thrombolysis* **2020**, *50*, 43–53.
[7] K. Thorlund, L. Dron, J. Park, G. Hsu, J. I. Forrest, E. J. Mills, *Lancet Digit. Heal.* **2020**, *2*, e286–e287.
[8] K. Damodharan, G. S. Arumugam, S. Ganesan, M. Doble, S. Thennarasu, *RSC Adv.* **2021**, *11*, 20006–20035.
[9] H. Xue, J. Li, H. Xie, Y. Wang, *Int. J. Biol. Sci.* **2018**, *14*, 1232–1244.
[10] N. E. Thomford, D. A. Senthebane, A. Rowe, D. Munro, P. Seele, A. Maroyi, K. Dzobo, *Int. J. Mol. Sci.* **2018**, *19*, DOI: 10.3390/ijms19061578.
[11] K. A. Bhakhar, N. D. Gajjar, K. B. Bodiwala, D. K. Sureja, T. M. Dhameliya, *J. Mol. Struct.* **2021**, *1244*, 130941.
[12] R. Chakravarti, R. Singh, A. Ghosh, D. Dey, P. Sharma, R. Velayutham, S. Roy, D. Ghosh, *RSC Adv.* **2021**, *11*, 16711–16735.
[13] T. F. Imbert, *Biochimie* **1998**, *80*, 207–222.
[14] C. C. Wen, Y. H. Kuo, J. T. Jan, P. H. Liang, S. Y. Wang, H. G. Liu, C. K. Lee, S. T. Chang, C. J. Kuo, S. S. Lee, C. C. Hou, P. W. Hsiao, S. C. Chien, L. F. Shyur, N. S. Yang, *J. Med. Chem.* **2007**, *50*, 4087–4095.
[15] M. Ono, Y. Nishida, C. Masuoka, J. C. Li, M. Okawa, T. Ikeda, T. Nohara, *J. Nat. Prod.* **2004**, *67*, 2073–2075.
[16] C. Y. Wei, S. W. Wang, J. W. Ye, T. L. Hwang, M. J. Cheng, P. J. Sung, T. H. Chang, J. J. Chen, *Molecules* **2018**, *23*, 2286.
[17] E. B. Rosmalena, Prasasty VD, Hanafi M, Budianto E, *Int. J. Pharm. Pharm. Sci.* **2015**, *7*, 394–398.
[18] M. Gordaliza, M. Castro, J. Miguel del Corral, A. San Feliciano, *Curr. Pharm. Des.* **2005**, *6*, 1811–1839.
[19] Q. Cui, R. Du, M. Liu, L. Rong, *Molecules* **2020**, *25*, 183.
[20] J. L. Charlton, *J. Nat. Prod.* **1998**, *61*, 1447–1451.
[21] P. R. Nagar, N. D. Gajjar, T. M. Dhameliya, *J. Mol. Struct.* **2021**, *1246*, 131190.
[22] N. D. Gajjar, T. M. Dhameliya, G. B. Shah, *J. Mol. Struct.* **2021**, *1239*, 130488.
[23] T. M. Dhameliya, P. R. Nagar, N. D. Gajjar, *Mol. Diversity* **2022**, DOI: 10.1007/s11030-022-10394–9.
[24] C. Gil, T. Ginex, I. Maestro, V. Nozal, L. Barrado-Gil, M. Á. Cuesta-Geijo, J. Urquiza, D. Ramírez, C. Alonso, N. E. Campillo, A. Martinez, *J. Med. Chem.* **2020**, *63*, 12359–12386.
[25] E. Eich, H. Pertz, M. Kaloga, J. Schulz, M. R. Fesen, A. Mazumder, Y. Pommier, *J. Med. Chem.* **1996**, *39*, 86–95.
[26] G. Liu, *Med. Chem.* **2009**, *5*, 29–43.
[27] V. Trinh Thi Thanh, V. Cuong Pham, H. Doan Thi Mai, M. Litaudon, F. Guéritte, P. Retailleau, V. H. Nguyen, V. M. Chau, *J. Nat. Prod.* **2012**, *75*, 1578–1583.
[28] Z. Yang, Y. Wang, Z. Zheng, S. Zhao, J. Zhao, Q. Lin, C. Li, Q. Zhu, N. Zhong, *Int. J. Mol. Med.* **2013**, *31*, 867–873.

[29] A. Martinez-Lopez, M. Persaud, M. P. Chavez, H. Zhang, L. Rong, S. Liu, T. T. Wang, S. G. Sarafianos, F. Diaz-Griffero, *EBioMedicine* **2019**, *47*, 269–283.
[30] H. W. Chen, J. X. Cheng, M. T. Liu, K. King, J. Y. Peng, X. Q. Zhang, C. H. Wang, S. Shresta, R. T. Schooley, Y. T. Liu, *Antiviral Res.* **2013**, *99*, 371–382.
[31] J. Li, A. P. Meng, X. L. Guan, J. Li, Q. Wu, S. P. Deng, X. J. Su, R. Y. Yang, *Bioorg. Med. Chem. Lett.* **2013**, *23*, 2238–2244.
[32] R. L. Huang, Y. L. Huang, J. C. Ou, C. C. Chen, F. L. Hsu, C. Chang, *Phyther. Res.* **2003**, *17*, 449–453.
[33] M.-J. Cheng, K.-H. Lee, I.-L. Tsai, I.-S. Chen, *Bioorg. Med. Chem.* **2005**, *13*, 5915–5920.
[34] S. Liu, W. Wei, K. Shi, X. Cao, M. Zhou, Z. Liu, *J. Ethnopharmacol.* **2014**, *155*, 1061–1067.
[35] R. Soto-Acosta, P. Bautista-Carbajal, G. H. Syed, A. Siddiqui, R. M. Del Angel, *Antiviral Res.* **2014**, *109*, 132–140.
[36] G. H. Syed, A. Siddiqui, *Hepatology* **2011**, *54*, 1936–1946.
[37] T. Merino-Ramos, N. Jiménez De Oya, J. C. Saiz, M. A. Martín-Acebes, *Antimicrob. Agents Chemother.* **2017**, *61*, e00376–17.
[38] H. J. Zhang, E. Rumschlag-Booms, Y. F. Guan, D. Y. Wang, K. L. Liu, W. F. Li, V. H. Nguyen, N. M. Cuong, D. D. Soejarto, H. H. S. Fong, L. Rong, *J. Nat. Prod.* **2017**, *80*, 1798–1807.
[39] S. Xu, N. Li, M. M. Ning, C. H. Zhou, Q. R. Yang, M. W. Wang, *J. Nat. Prod.* **2006**, *69*, 247–250.
[40] X. yan Qu, Q. jun Li, H. min Zhang, X. juan Zhang, P. hui Shi, X. juan Zhang, J. Yang, Z. Zhou, S. qi Wang, *Arch. Pharmacal Res.* **2016**, *39*, 998–1005.
[41] C. W. Chang, M. T. Lin, S. S. Lee, K. C. S. C. Liu, F. L. Hsu, J. Y. Lin, *Antiviral Res.* **1995**, *27*, 367–374.
[42] Y. Qian Liu, L. Yang, X. Tian, *Curr. Bioact. Compd.* **2007**, *3*, 37–66.
[43] M. Chen, N. Kilgore, K. H. Lee, D. F. Chen, *J. Nat. Prod.* **2006**, *69*, 1697–1701.
[44] Y. Xue, X. Li, X. Du, X. Li, W. Wang, J. Yang, J. Chen, J. Pu, H. Sun, *Phytochemistry* **2015**, *116*, 253–261.
[45] X. Y. Xu, D. Y. Wang, C. F. Ku, Y. Zhao, H. Cheng, K. L. Liu, L. J. Rong, H. J. Zhang, *Chin. J. Nat. Med.* **2019**, *17*, 945–952.
[46] K. Fanhchaksai, K. Kodchakorn, P. Pothacharoen, P. Kongtawelert, *Vitr. Cell. Dev. Biol. - Anim.* **2016**, *52*, 107–119.
[47] J. Wagoner, A. Negash, O. J. Kane, L. E. Martinez, Y. Nahmias, N. Bourne, D. M. Owen, J. Grove, C. Brimacombe, J. A. McKeating, E. I. Pécheur, T. N. Graf, N. H. Oberlies, V. Lohmann, F. Cao, J. E. Tavis, S. J. Polyak, *Hepatology* **2010**, *51*, 1912–1921.
[48] J. H. Song, H. J. Choi, *Phytomedicine* **2011**, *18*, 832–835.
[49] J. J. Pollara, S. M. Laster, I. T. D. Petty, *Antiviral Res.* **2010**, *88*, 287–295.
[50] H. Chen, L. Teng, J. N. Li, R. Park, D. E. Mold, J. Gnabre, J. R. Hwu, W. N. Tseng, R. C. C. Huang, *J. Med. Chem.* **1998**, *41*, 3001–3007.
[51] J. N. Gnabre, J. N. Bradyt, D. J. Clantont, Y. Ito, J. Dittmert, R. B. Bates, R. Chih, C. Huang, *Biochemistry* **1995**, *92*, 11239–11243.
[52] X. N. Li, J. X. Pu, X. Du, L. M. Yang, H. M. An, C. Lei, F. He, X. Luo, Y. T. Zheng, Y. Lu, W. L. Xiao, H. D. Sun, *J. Nat. Prod.* **2009**, *72*, 1133–1141.
[53] Y. C. Kuo, Y. H. Kuo, Y. L. Lin, W. J. Tsai, *Antiviral Res.* **2006**, *70*, 112–120.
[54] "Dassault Systèmes BIOVIA, BIOVIA Workbook, Release **2021**; BIOVIA DS Visualizer, Release **2021**, San Diego: Dassault Systèmes, **2021**.".
[55] T. M. Dhameliya, K. I. Patel, R. Tiwari, S. K. Vagolu, D. Panda, D. Sriram, A. K. Chakraborti, *Bioorg. Chem.* **2021**, *107*, 104538.
[56] T. M. Dhameliya, A. A. Devani, K. A. Patel, K. C. Shah, *ChemistrySelect* **2022**, *7*, e202200921.
[57] T. M. Dhameliya, S. J. Chudasma, T. M. Patel, B. P. Dave, *Mol. Diversity* **2022**, DOI: 10.1007/s11030-021-10375–4.
[58] K. A. Bhakhar, D. K. Sureja, T. M. Dhameliya, *J. Mol. Struct.* **2022**, *1248*, 131522.
[59] T. M. Dhameliya, K. A. Bhakhar, N. D. Gajjar, K. A. Patel, A. A. Devani, R. V. Hirani, *J. Mol. Struct.* **2022**, *1248*, 131473.
[60] S. J. Chudasama, B. J. Shah, K. M. Patel, T. M. Dhameliya, *J. Mol. Liq.* **2022**, *361*, 119664.
[61] A. Kumar, T. M. Dhameliya, K. Sharma, K. A. Patel, R. V. Hirani, *ChemistrySelect* **2022**, *7*, e202201059.
[62] A. Kumar, T. M. Dhameliya, K. Sharma, K. A. Patel, R. V. Hirani, A. J. Bhatt, *J. Mol. Struct.* **2022**, *1259*, 132732.
[63] T. M. Dhameliya, P. R. Nagar, K. A. Bhakhar, H. R. Jivani, B. J. Shah, K. M. Patel, V. S. Patel, A. H. Soni, L. P. Joshi, N. D. Gajjar, *J. Mol. Liq.* **2022**, *348*, 118329.
[64] C. A. Lipinski, F. Lombardo, B. W. Dominy, P. J. Feeney, *Adv. Drug Delivery Rev.* **2001**, *46*, 3–26.
[65] M. F. Khan, G. Verma, W. Akhtar, M. Shaquiquzzaman, M. Akhter, M. A. Rizvi, M. M. Alam, *Arab. J. Chem.* **2019**, *12*, 5000–5018.
[66] M. Q. Zhang, B. Wilkinson, *Curr. Opin. Biotechnol.* **2007**, *18*, 478–488.
[67] "pkCSM: Pharmacokinetic properties," can be found under http://biosig.unimelb.edu.au/pkcsm/prediction, (accessed on Septemeber 19, **2021**).
[68] D. E. V. Pires, T. L. Blundell, D. B. Ascher, *J. Med. Chem.* **2015**, *58*, 4066–4072.
[69] A. Daina, O. Michielin, V. Zoete, *Sci. Rep.* **2017**, *7*, 42717.
[70] D. F. Veber, S. R. Johnson, H. Y. Cheng, B. R. Smith, K. W. Ward, K. D. Kopple, *J. Med. Chem.* **2002**, *45*, 2615–2623.
[71] W. J. Egan, K. M. Merz, J. J. Baldwin, *J. Med. Chem.* **2000**, *43*, 3867–3877.
[72] I. Muegge, S. L. Heald, D. Brittelli, *J. Med. Chem.* **2001**, *44*, 1841–1846.
[73] A. K. Ghose, V. N. Viswanadhan, J. J. Wendoloski, *J. Comb. Chem.* **1999**, *1*, 55–68.
[74] J. D. Durrant, J. A. McCammon, *BMC Biol.* **2011**, *9*, 71.
[75] A. Hospital, J. R. Goñi, M. Orozco, J. L. Gelpí, *Adv. Appl. Bioinforma. Chem.* **2015**, *8*, 37–47.
[76] M. González Torres, E. Villarreal-Ramírez, M. de los A. Moyaho Bernal, M. Álvarez, J. González-Valdez, J. A. Gutiérrez Uribe, G. Leyva Gómez, J. R. C. Cortez, *J. Mol. Struct.* **2019**, *1175*, 536–541.
[77] T. C. Ramalho, T. C. C. França, W. A. Cortopassi, A. S. Gonçalves, A. W. S. Da Silva, E. F. F. Da Cunha, *J. Mol. Struct.* **2011**, *992*, 65–71.
[78] S. Abbas, H. H. Nasir, S. Zaib, S. Ali, T. Mahmood, K. Ayub, M. N. Tahir, J. Iqbal, *J. Mol. Struct.* **2018**, *1156*, 193–200.
[79] R. Z. Batran, M. A. Khedr, N. A. Abdel Latif, A. A. Abd El Aty, A. N. Shehata, *J. Mol. Struct.* **2019**, *1180*, 260–271.
[80] P. Modi, S. Patel, M. Chhabria, *Bioorg. Chem.* **2019**, *87*, 240–251.
[81] V. Hornak, C. Simmerling, *J. Mol. Graphics Modell.* **2004**, *22*, 405–413.
[82] M. J. Abraham, Berk Hess, E. Lindahl, D. van der Spoel, "GROMACS 2020.1 (Manual Version 2020.1) Zenodo," can be found under http://doi.org/10.5281/zenodo.4054996, **2020**.
[83] M. J. Abraham, T. Murtola, R. Schulz, S. Páll, J. C. Smith, B. Hess, E. Lindah, *SoftwareX* **2015**, *1–2*, 19–25.

Submitted: May 28, 2022
Accepted: July 5, 2022